Proceedings of ASME 2011 5th International Conference on Energy Sustainability & 9th Fuel Cell Science, Engineering and Technology Conference
ESFuelCell2011
August 7-10, 2011, Washington, DC, USA

ESFuelCell2011-54295

SIMULATION OF FLOW INSIDE HEAT PIPE: SENSITIVITY STUDY, CONDITIONS AND CONFIGURATION

Nouman Zahoor Ahmed
Masdar Institute of Science and Technology
Abu Dhabi, U.A.E.

Pawan K. Singh
Masdar Institute of Science and Technology
Abu Dhabi, U.A.E.

Isam Janajreh
Masdar Institute of Science and Technology
Abu Dhabi, U.A.E.

Youssef Shatilla
Masdar Institute of Science and Technology
Abu Dhabi, U.A.E.

ABSTRACT

Heat pipes are widely used as a heat transporting device in a variety of applications. From space satellites, large industrial appliances to a heat sink for cooling electronic components and packages. Heat pipes are extremely efficient because of their high effective thermal conductivity, compactness, low cost and reliability. Therefore, the designers of heat sinks are often required to optimize the performance of the heat pipe itself in order to improve the overall thermal management system of any particular equipment. However, the detailed internal modeling of a heat pipe presents a challenging problem for an engineer. It is a multi physics problem including two phase flow within porous media and with conjugate heat transfer adding the solicited high capillary and surface tension effect.

In this present study, detailed modeling of the heat pipe considering the mentioned effects is pursued. A basic review of the governing equations describing the complete heat pipe operation is given. The commercially available simulation tool Fluent 6.3 is used to describe and solve these equations in a coupled conjugate heat transfer set up. The geometry of heat pipe is divided in two different regions which solve simultaneously. The first region is core region where only vapor flow is assumed. The second region consists of wall and wick structure through which the mass transfer due to wettability and heat dissipates through conduction. Water was used as flowing fluids through wick porous structure. Previous experimental as well as numerical models regarding the heat pipes have been studied and used for the verification of the present model along with a standard grid convergence study. The effects of different heat pipe length, heat fluxes, wall thickness, wall material and porosity are investigated. The pressure drop and wall temperature increase with the value of heat flux. Similarly, porosity and wall material affect the wall temperature distribution. The effect of wall thickness and heat pipe length was not significant. In addition, a theoretical model is developed for the pressure drop across the heat pipe in vapor region and the respective output was used for the simulation. Finally, the temperature distribution in wall and wick is shown and discussed.

NOMENCLATURE:

A	Cross-sectional area, m^2
h	Characteristic dimension (half width or radius), m
h_{fg}	Latent heat of vaporization, J/kg
k	Thermal conductivity
K(R)	Constant of integration
L	Length, m
L_{eff}	Effective length of the heat pipe, m^2
$\dot{m}$	Mass flow rate, kg/s
P	Pressure, Pa
ΔP	Pressure drop, Pa
Q	Heat Flux, W
Q_{max}	Maximum heat flux, W/m^2
R_c	Radius of curvature, m
r_p	Radius of capillary or pore, m
T	Temperature, K
u	Coordinate in the vertical (radial) direction of heat pipe
x	Coordinate in the vertical (radial) direction of heat pipe
y	Coordinate in the vertical (radial) direction of heat pipe
μ	Dynamic viscosity, $N.s/m^2$
ρ	Density, kg/m^3
Ø	Tilt angle, Radians
λ	Dimensionless radial coordinate
K	Permeability, m^2
∇	Divergence
σ	Surface tension, N/m

Subscripts

a	adiabatic section, axial
c	condenser, capillary
e	evaporator

INTRODUCTION

Although heat pipe was invented much earlier, its application in the electronics thermal management started around 1990's [1]. Perhaps the drive towards miniaturization and increasing processing capacity for the electronics has been the fundamental demand where heat pipes serves extremely well as they can transfer large amount of heat from a heat source to heat sink effectively. Since then it has become an integral part of the heat sink mechanism for numerous devices. Fig. 1 shows a typical cylindrical heat pipe similar to the one that has been chosen for our present study.

Previously several theoretical and experimental work has been conducted with the aim of analyzing the fluid behavior inside the heat pipe so as to optimize the device for maximizing the heat transport. Thermal resistance network analysis for a heat pipe has been used successfully to estimate the temperature drop for a given heat flux. Peterson [2] has used this approach to optimize heat pipe cooling device for mobile computers by comparing two different prototypes where the maximum heat transport capacity for any heat pipe is limited by the fundamental wicking or capillary limitation along with sonic, entrainment and boiling limitations as given in various references [3][4].

Faghri [5] and Layeghi [6] have given a detailed numerical model for the vapor flow analysis in a concentric annular heat pipe. Similarly, a detailed review discussing the design, modeling, limitations and testing procedures has been performed by Borujerdi and Layeghi [7]. Relying on the velocity correlations derived through these studies for concentric annular heat pipes, Shoeib & Mahtabroshan [8] have performed a CFD simulation for a cylindrical heat pipe as well. However it is possible to perform the heat pipe CFD analysis by using less strict and different boundary conditions suited to optimize the device under different working conditions.

Peterson [3] has described pressure distribution within the heat pipe in detail using analytical experimental or numerical simulation. The capillary pressure developed at the liquid interface and its variation along the length of the heat pipe is described in detail. The vapor pressure distribution has also been studied by Leong [9] for a flat

heat pipe. The appropriateness of these pressure correlations as a boundary condition for the CFD simulations and the associated velocities has also been addressed in this work.

As the area of current interest is the use of heat pipe for optimizing the microprocessor cooling in laptops and typical heat sinks in laptops usually have one more heat pipe arranged with very little or no inclination angle. Therefore the gravity effects have not been considered in this analysis.

In the present study, effort has been made to simulate the heat pipe mechanism with the actual temperature conditions that a heat pipe is subjected to in a typical notebook computer for example. Reference values have been selected from data obtained through latest processor specifications available on the Intel website [14].

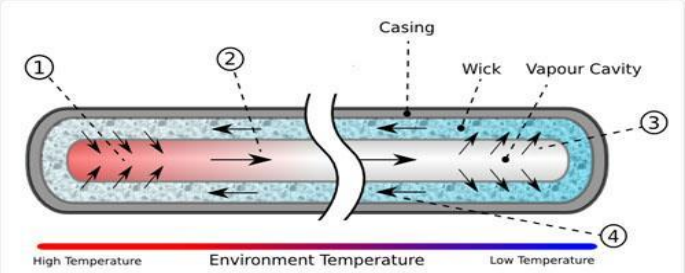

Figure1. Illustration of heat pipe and its components (evaporator section, adiabatic/convicted section, and condenser section)

GOVERNING EQUATIONS

The governing equations that describe the behavior of heat pipe are those which govern mass, momentum and energy conservation. That is,

Conservation of Mass (continuity equation)

$$\frac{d\rho}{dt} + \rho(\bar{\nabla}.\bar{V}) = 0 \qquad (1)$$

Conservation of momentum (Newton's second law of momentum) or Navier Stokes Equation of fluid motion,

$$\rho\frac{D\bar{V}}{Dt} = -\bar{\nabla}P + \rho\bar{g} + \mu\nabla^2\bar{V} \qquad (2)$$

Conservation of Energy

$$\rho C_v\frac{DT}{Dt} = -P\bar{\nabla}.\bar{V} + \kappa\nabla^2 T - \bar{\nabla}.\bar{q_r} + q''' + \Phi \qquad (3)$$

Where ∇ or "Del" is called the divergence

Φ = dissipation function

q''' = internal heat generation rate per unit volume

q_r = radiation heat flux

The pressure drop through the porous medium follows Darcy's law [10]:

$$\Delta P_l = \frac{\mu_l L_{eff}\,\dot{m}}{\kappa\rho_l A_w} \qquad (4)$$

Finite volume based approach is used in this study. The simulations have been performed using Fluent 6.3. The system dimensions are supposed to follow continuum and hence the macroscopic properties of fluids are considered for the analysis.

Pressure Distribution inside a heat pipe

For any heat pipe, the difference in capillary pressures at the liquid vapor interface between evaporator and condenser is given by Peterson [3],

$$\Delta P_c = \frac{2\sigma}{R_{c,e}} - \frac{2\sigma}{R_{c,c}} \qquad (5)$$

And the maximum capillary pressure generated inside heat pipe is,

$$\Delta P_{c,\max} = \frac{2\sigma}{R_{c,e}} \qquad (6)$$

Where $R_{c,e}$ becomes the radius of the pore at the evaporator. At this condition and according to the standard steady state working condition for any heat pipe,

$$\Delta P_c - \Delta P_g = \Delta P_l + \Delta P_v \qquad (7)$$

Where ΔP_g is the gravitational head, the vapor phase pressure drop ΔP_v can be neglected and the liquid phase pressure drop, ΔP_l is given by Darcy's Law Eq. (4). Hence by using the relationship $Q_{\max} = m_{\max} h_{fg}$ and putting in the values from Eq. (6) and Eq. (4) into Eq. (7) the maximum amount of heat flux that a heat pipe can transport is given by [4],

$$Q_{\max} = \left(\frac{\rho_l\sigma h_{fg}}{\mu_l}\right)\left(\frac{A_w\kappa}{L_{eff}}\right)\left(\frac{2}{r_p} - \frac{\rho_l\, g\, L_{eff}\sin\phi}{\sigma}\right) \qquad (8)$$

The variation of surface tension "σ" between the liquid water and vapor at specified pressure is available through literature. However, the variation of the radius of curvature "R_c" that affects the capillary pressure depends not only upon the pore size and temperature but also on the saturation level of wetting fluid inside the porous medium [11].

Hence various mathematical formulations have been made to show the general pressure distribution inside a heat pipe by simplifying the momentum equations substituting velocity with heat flux values associated with the latent heat [9] such that:

$$V = \frac{Q}{\rho A h_{fg}} \tag{9}$$

The theoretical correlations developed by Leong [9] for a flat heat pipe can be used to predict the vapor pressure distribution by replacing the characteristic dimension "h" from half width to the radius for a conventional cylindrical heat pipe.

$$P(x,\lambda) = P(0,\lambda) + \frac{\mu}{h^3} V_e \frac{x^2}{2} k(R) \tag{10}$$

$$0 \le x \le L_e$$

$$P(x,\lambda) = P(L_e,\lambda) + \frac{\mu}{h^2} 2\overline{u_a}(x - L_e) k(R) \tag{11}$$

$$L_e \le x \le L_e + L_a$$

$$P(x,\lambda) = P(L_e + L_a,\lambda) + \frac{\mu}{h^3} V_c k(R)\left[(Lx - \tfrac{1}{2}x^2) - \tfrac{1}{2}(L^2 - L_c{}^2)\right]$$

$$L_e + L_a \le x \le L \tag{12}$$

By the above equation, the pressure at the condenser end can be given as-

$$P(L,\lambda) = P(0,\lambda) + \frac{\mu}{h^3} V_e \frac{L_e^2}{2} + \frac{\mu}{h^2} 2\overline{u_a} L_a + \frac{\mu}{h^3} V \frac{L_c^2}{2}{}_c \tag{13}$$

Hence by adding these individual pressures the total vapor pressure difference between the start of the evaporator and the condenser end can be given as,

$$\Delta P = P(L,\lambda) - P(0,\lambda)$$

$$= \frac{\mu}{h^3} V_e \frac{L_e^2}{2} + \frac{\mu}{h^2} 2\overline{u_a} L_a + \frac{\mu}{h^3} V \frac{L_c^2}{2}{}_c \tag{14}$$

The substitution for the inlet radial velocities, V_e, V_c, and the average axial velocity $\overline{u_a}$ in the above equation and further simplification yields the following results,

$$\Delta P = \frac{\mu Q}{\rho h^2 h_{fg}} \times \left[\frac{1}{A_e} \frac{L_e{}^2}{2} + \frac{2L_a}{A_a} + \frac{1}{2hA_c} L_c{}^2 \right] \text{ or}$$

$$\Delta P = \frac{\mu Q}{\rho h^2 h_{fg}} \times C_1 \tag{15}$$

The calculated value for constant C_1 according to the parameters given in the Table 1 gives,

$$\Delta P = 3294 \times \left(\frac{\mu Q}{\rho h^2 h_{fg}} \right) \tag{16}$$

For different values of heat flux, the associated pressure drops and the radial velocities are given in the tabulated form in Table 1.

NUMERICAL MODEL DETAILS

Numerical simulations of the descritized equation (1-3) have been performed in CFD software package, Fluent 6.3.26 under 2D, double precision axi-symmetric conditions to take advantage of the symmetry for cylindrical heat pipe. Fig 1 and Fig 2 shows the front and the side view of the geometry with the details and specifications listed in Table 2.

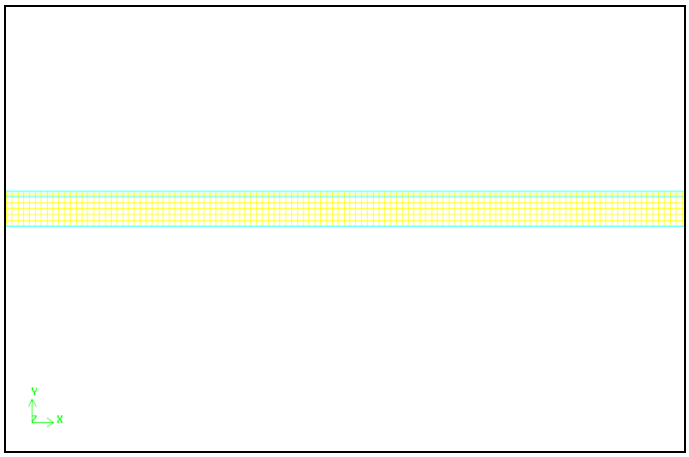

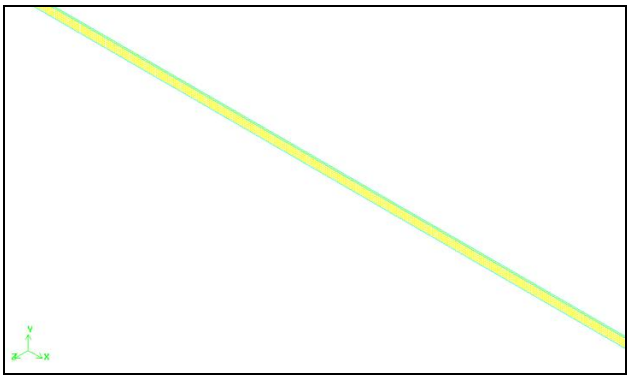

FIG 2. The geometry of heat pipe with mesh

Flux (Watts)	Vapor Pressure Drop (Pa)	Velocity at evaporator Inlet (m/s)
81	0.1495	0.096
108	0.1992	0.127
135	0.2490	0.159

Table 1: Pressure drop with available heat dissipation

Parameter	**Value**
Total length	0.2 m
Evaporator	0.025 m
Adiabatic Section	0.115 m
Condenser	0.06 m
Wick thickness	0.15e-3 m
Wall thickness	0.75e-3 m
Inner core radius	4e-3 m
Saturated Temperature	323 K
Water density	1000 kg/m^3
Vapor density	0.5974 kg/m^3
viscosity	121e-7 Pa.sec
h_{fg}	2260 KJ/kg

Table 2: Details of heat pipe with properties values.

INITIAL AND BOUNDARY CONDITIONS

For a heat pipe, typical boundary conditions include the isothermal temperature conditions at the evaporator and condenser section. This can be replaced with the constant heat flux condition at one or both of these sections such that:

Outer evaporator wall: constant heat flux
Outer condenser wall: constant heat flux
Outer adiabatic section wall: natural convection

Typically heat flux values for processors ranges between 50 to 100 Watts [12]. Considering an average chip size of 3X3 cm^2, this translates into the flux values between 50,000 to 100,000 Watts per cubic meters roughly. Reference flux values given in table 1 are selected keeping in view the above mentioned considerations. However, localized flux on the silicon chip may rise quite significantly up to 1,000 Watts per cm^2 and this requires novel cooling techniques as discussed by [13]

At the interface between wick and vapor section, Clausisus clayperon equation describes the temperature conditions.

$$T_{\text{int}} = \frac{1}{\frac{1}{T_{v,sat}} - \frac{R}{h_{fg}} \ln \frac{P_v}{P_{v,sat}}} \qquad (17)$$

Corresponding to the different flux values, inputs from Table 1 have been used to capture the fluid motion and pressure drop effects.

Since the thickness of the heat pipe is very small as compared to the length hence the heat losses from the sides can be assumed as negligible. Constant heat source and heat sink are added to incorporate the effect of latent heat.

Heat pipe analysis is carried out under steady state conditions.

VALIDATION OF NUMERICAL SCHEME

Figure 3 shows the pressure variation inside the core vapor region. The vapor pressure distribution conforms to the general trend shown by the previous experimental, studies conducted by Faghri and Layeghi for concentric annular heat pipe which showed the comparison of normalized pressure distribution [5] [6]. Here, the values are not compared since the geometries for both the analysis were different. The trend shows a nonlinear pressure drop in evaporator section which is due to the change in velocity. In the adiabatic region, pressure drop is linear; demonstrating that the velocity in this region is in axial direction with constant value. The condenser

region again shows the increase in pressure drop due to decrease in velocity. Here the present graph differs from the results of Faghri et. al. [5] because the values selected for Radial Re number in their study were very low, which made the velocity in condenser region almost constant and hence no significant pressure drop was observed, while our present study is done for moderate radial Re and so the pressure try to recover in condenser section. This increase is again nonlinear due to same reason given for the evaporator. The solution has been checked with three different grids with 1407 nodes, 3000 nodes and 5213 nodes.

	No. of nodes	Variable	Error %
1	1407	Vapor Pressure	-
2	3000	Vapor Pressure	2
3	5213	Vapor Pressure	0.5

Table 3: Grid sensitivity analysis

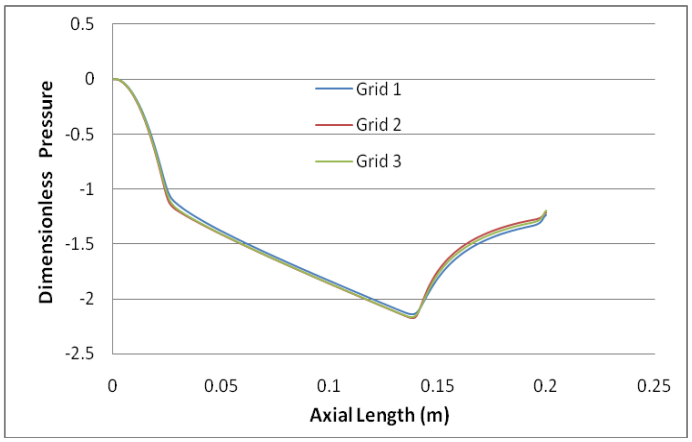

FIGURE 3. Grid sensitivity study.

It is found that the change in vapor pressure distribution is less than 0.5 % while increasing the number of nodes from 1407 to 5213 nodes. Hence the core vapor region is solved with 5213 nodes. Similarly for wall-wick region also, the grid independence test is carried out and it is found that 4207 nodes are sufficient to carry out the simulation. The mesh scheme adopted for both the regions was quadrilateral mesh.

Results and Discussion:

The working and efficiency of heat pipe depend on a lot of parameters like length, radius, material, heat dissipated, wick structure etc. The following section shows the effect of these parameters one by one.

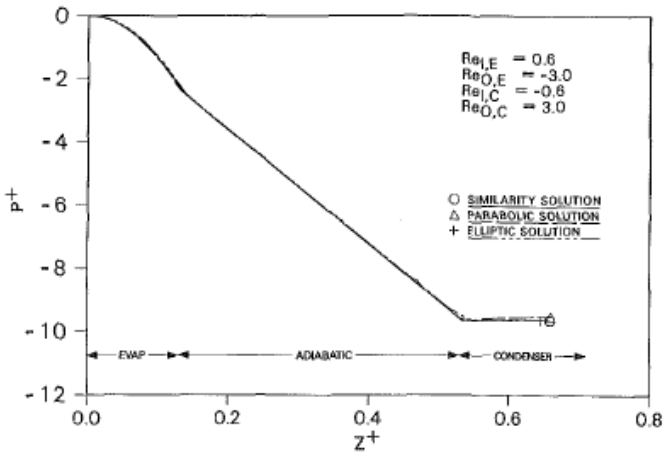

FIGURE 4 (A). Validation of numerical scheme with avaiable results.

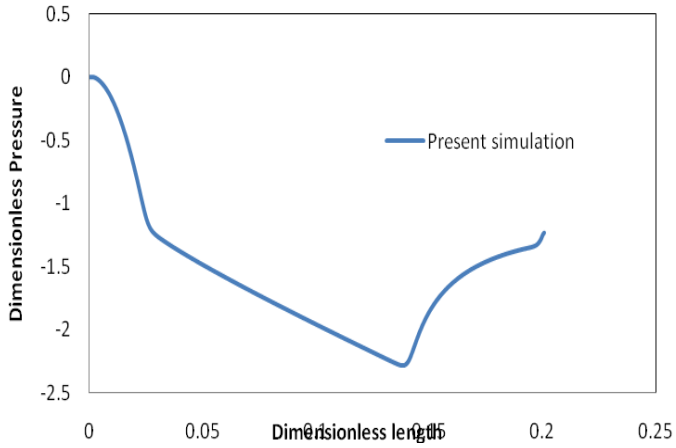

FIGURE 4(B). Validation of numerical scheme with avaiable results.

a. Pipe length

Since in a heat pipe, the length of evaporator and condenser cannot be changed due to geometric consideration, the length of heat pipe can be changed only by changing adiabatic length. Fig. 5 describes the variation of wall temperature for different lengths of heat pipe. The variation of wall temperature is shown for three different heat pipe lengths, 0.2 m, 0.225 m and 0.25 m. It can be seen here, the trend and values of wall temperature does not change with different heat pipe length. Only they shift according to adiabatic length. The probable

reason for this behavior lies in the basic heat transfer mechanism of heat pipe. Since the heat dissipated through evaporator and condenser is not changed and the heat transfer through adiabatic part is negligible, the trend of wall temperature remains constant with different heat pipe length.

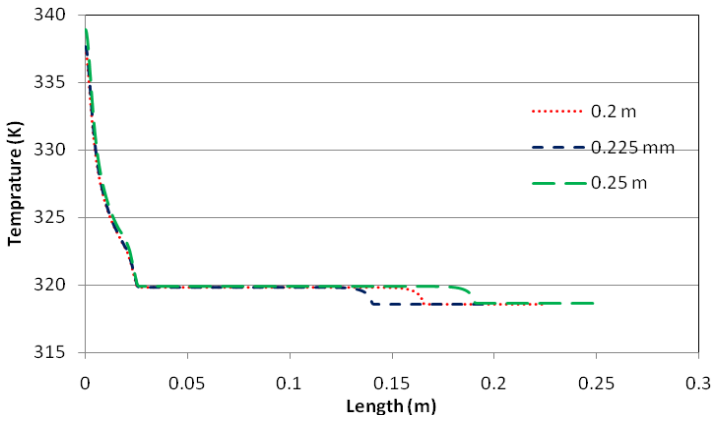

FIGURE 5 Wall temperatures against different Pipe length

b. Wall diameter

The change in pipe diameter will change the surface area available for heat transfer. The variation of wall temperature with wall thickness is shown in Fig. 6. Three wall thickness, 0.15 mm, 0.25mm and 0.35 mm are taken for analysis and it can be seen from fig. 6 that the change in variation of wall temperature with wall thickness is negligible. It shows that the conduction heat transfer through wall does not change much with wall thickness.

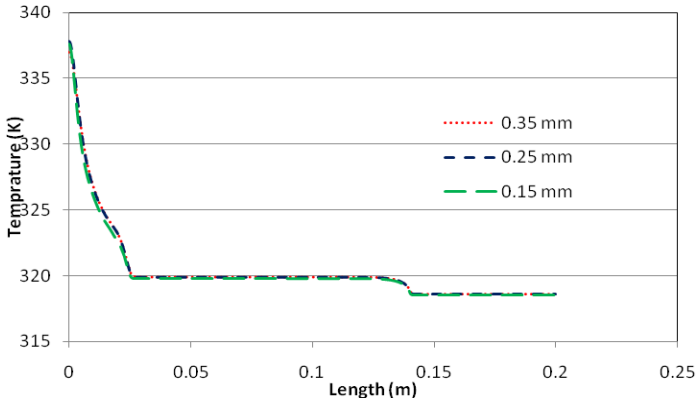

FIGURE 6 Wall temperatures against different Pipe length

c. Heat flux

Fig. 7 shows the temperature variation at wall against length of heat pipe for different values of powers. The value takes are actual and taken from INTEL [14]. It can be seen here that the trend of temperature is same for all the fluxes. The evaporator section wall shows a steep variation in wall temperature, indicating that the maximum heat transfer occur in the evaporator section. It is expected, since to simulate the real condition, a heat source is added in the evaporator section in addition of normal steady heat conduction. The values of temperatures are constant in adiabatic section. Since the heat transfer from this section is only through natural convection, so the heat dissipated through this section is low and does not make any change in the temperature. The condenser region also shows the same trend as adiabatic section except that it is at lower values than that of adiabatic region. The mechanism of heat transfer in this section is force convection. This makes the heat transfer better compared to adiabatic section, but it is still not enough to make any significant change in variation of temperature. As expected, the temperature is highest for the 135 watt power and lowest for the 75 W powers. It clearly demonstrate that the maximum heat transfer and so the wall temperature occur with maximum power.

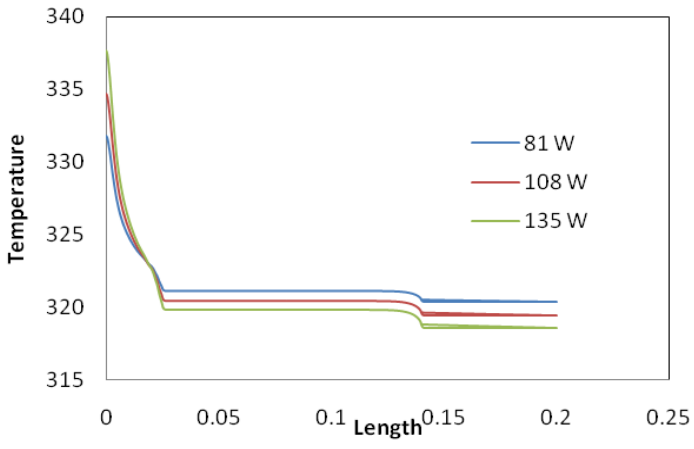

FIGURE 7. Wall temperature against Pipe length with different heat

d. Porosity

The effect of porosity on the variation of temperature is also investigated. Fig. 8 is plotted by considering three different wick structures having different porosity for same heat flux. Here also the nature of graphs is same as figure 7.

It is clearly visible that the values of wall temperature are higher with higher porosity and lowest for the lowest porosity of wick in evaporator wall. It means that the heat pipe with lower porosity is better. In other words, the void fraction should be lower and mesh in wick will be having more solid region. This will help in increasing capillary pressure and flow will be easy. But at the same time, it will decrease mass flow rate due to less space available for flow and hence decrease the heat dissipation. There is a need of optimum porosity to get maximum heat dissipation. Also the change in the wall temperature is very steep with porosity.

e. Wall material

The following graph shows the effect of wall material on distribution of temperature. It is a well known fact [3] that we cannot choose the wall and liquid materials. Their compatibility needs to be checked before using them. From the literature, [3] three most common wall materials; Copper, Aluminum and Steel are chosen. It can be seen from Fig. 9 that the wall temperature varies significantly with wall material. The values of temperature are the highest for Steel and the lowest for Copper. The reason for this difference lies in the thermal conductivity of the material used. The value of thermal conductivity is highest for Copper and lowest for Steel. Also the difference in the values of thermal conductivity is of one order for Steel and Copper and so the values of wall temperature are maximum for Steel and lowest for Copper.

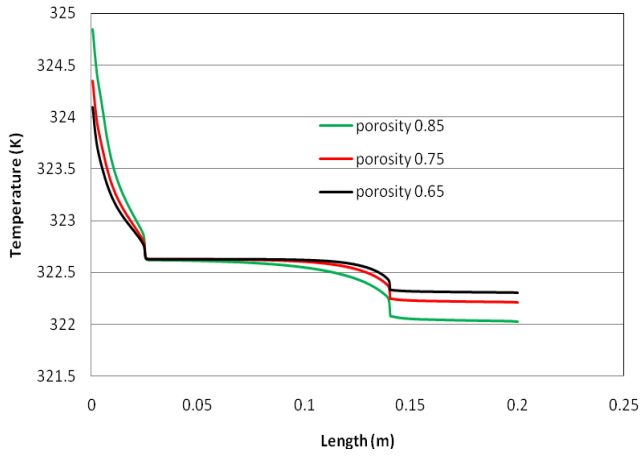

FIGURE 8. Wall temperature against Pipe length with different values of porosities

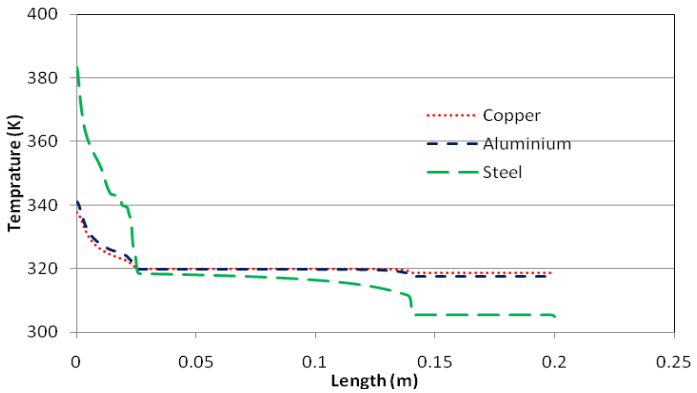

FIGURE 9. Wall temperature against different wall material

Figure 10 shows the axial distribution of vapor pressure for different heat flux along the length of heat pipe. It can be seen here that the variation of pressure is highest for the maximum heat flux. This is expected, since to co-up

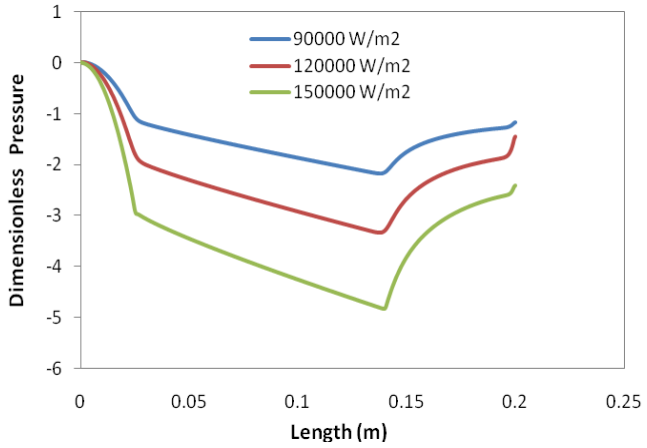

FIGURE 10. Pressure distribution in vapor region with different heat flux

with high heat dissipation the flow area needs to be increased and hence the pressure drop.

Figure 11 shows the temperature distribution inside the wick and wall structure for three different heat flux. As expected the values of temperature is highest for higher heat flux. The contour also shows that the values of temperature is higher towards wall and it decrease axially. The value of temperatures decreases also towards y axis. This shows that the heat transfer is in both directions. Also these heat transfers are mainly due to conduction inside the wall and wick.

CONCLUSION

In this work the numerical analysis of heat pipe is carried out. The governing mass, momentum and energy equation for conjugate heat transfer are descritized and solved using Fluent 6.3 commercial code. The geometry is divided in two regions. First one is core region through which vapor flows and second one is wall wick region. In addition, the equation for pressure drop in vapor region is developed and the inputs for numerical model are taken from this analysis. The effects of various parameters like heat flux, porosity, wall thickness, pipe length and wall material are discussed. The variation of wall temperature with different pipe lengths and wall thickness was not significant. It is found that the wall temperature increases with heat flux. The porosity plays a major role in heatpipe and as it increases temperature of the evaporator decreases. The material of wall is an important concern while designing the heat pipe since it changes significantly the variation of wall temperature. From the theoretical analysis, it is found that pressure drop across the vapor region increases with higher heat dissipation. The temperature distribution in the wall and wick region is shown. The regions, vapor and wall-wick are coupled through velocity. Still they are now coupled directly and solved separately. The further analysis is going on to make the heat pipe simulation more real and accurate.

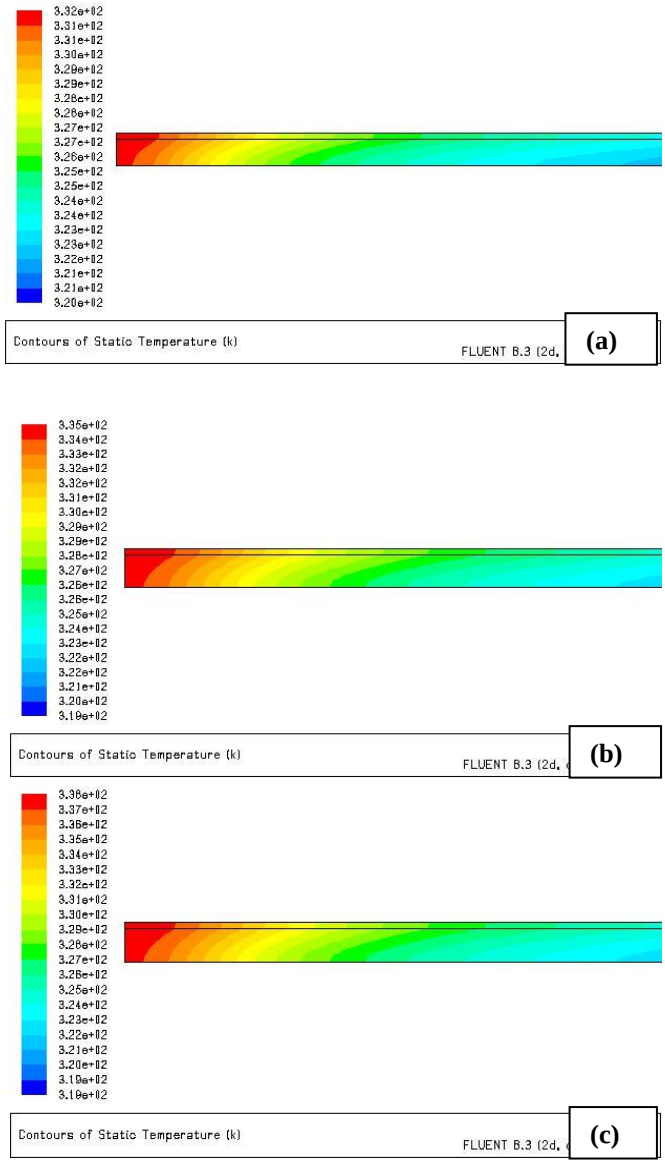

FIGURE 11. Temperature distributions inside wall and wick for different heat flux (a) 90, (b) 120 and (c) 150 kW/m^2.

ACKNOWLEDGEMENTS

The financial support from Masdar Institute to carry this work is highly acknowledged. The author would like to extend his gratitude for the help and support received from the Waste to Energy Group at Masdar Institute.

REFERENCES

[1] Scott D. Garner, September 1, 1996, "Heat Pipes for Electronics Cooling Applications", *Electronics Cooling.*

[2] Y. Wang, G. P. Peterson, 2003, "Flat Heat Pipe Cooling Devices for Mobile Computers", *Proceedings of ASME International Mechanical Engineering Congress*, Washington, D. C.

[3] G. P. Peterson, 1994, *An Introduction to Heat Pipes Modelling, Testing and Applications*, John Wiley & Sons Inc., NY.

[4] A. F. Mills, 1999, *Heat Transfer*, Prentice Hall Inc., NJ.

[5] A. Faghri, 1989, "Performance characteristics of a concentric annular heat pipe: Part II- vapor flow analysis", *Journal of Heat Transfer* Vol. (111).

[6] A. Borujerdi & M. Layeghi, 2004, "Numerical Analysis of Vapor Flow in Concentric Annular Heat Pipes", *Journal of Heat Transfer* Vol. (126).

[7] A. Borujerdi, M. Layeghi, 2005, "A Review of Concentric Annular Heat Pipes", *Heat Transfer Engineering*, Vol. (26), No. 6,

[8] S. Mahjoub & A. Mahtabroshan, 2008, "Numerical Simulation of a conventional heat pipe", *World Academy of Science, Engineering and Technology* Vol. (39).

[9] K. C. Leong, C. Y. Leong, 1996, "Vapor Pressure Distribution of a Flat Heat Pipe", *Int. Comm. Heat Mass Transfer*, Vol. (23), No. 6, pp. 789-797.

[10] James A. Fay, 1994, *Introduction to Fluid Mechanics*, The MIT Press.

[11] G. F. Pinder, W. G. Gray, 2008, *Essentials of Multiphase Flow and Transport in Porous Media*, John Wiley and Sons Inc., NJ

[12] Intel corporation website: http://www.intel.com/products/processor/index.htm, last visited in Jan 2011.

[13] A. B. Cohen, P. Wang, 2009, "Thermal management of on-chip hot spot"**,** *Proceedings of 2nd Micro/Nanoscale Heat and Mass Transfer International Conference.*

[14] Fluent Inc.*, "Fluent 6.3 Users Guide"* 2006.